Influence of Simple Harmonic Speed Variations on the Vuk-T Sailplane Approach Paths and Distances

Zoran Stefanović
Professor

Ivan Kostić
Assistant Professor

Faculty of Mechanical Engineering
University of Belgrade

When for any technical reason spoilers become inoperable in flight, the most critical phase of a sailplane landing procedure is final approach. Besides the sideslipping flight possibility, where energy is dissipated through the increased sideforce drag, another solution for this problem has been offered in literature, showing that the landing distance could be minimized using rather complex oscillating flight paths. The problem is that performing such paths in practice would require exceptional piloting skills. Instead of that, in this paper much simpler approach profiles have been analyzed, based on the simple harmonic speed variations, which could much easier be reproduced in practice. After establishing a quick convergence algorithm, numerical solutions for several typical cases, taking the Vuk-T sailplane as an example, have been presented. Although distance reductions are generally smaller than obtained by distance-minimizing techniques, their operational simplicity and higher safety prove them as valuable solutions for this kind of problems.

Keywords: *sailplane, inoperable spoilers, harmonic speed variation, landing approach, distance reduction*

1. INTRODUCTION

High lift-to-drag ratios of the contemporary sailplanes enable them to fly very long distances from a given height or stay in the air for a very long time without an engine, making them the most energy efficient flying vehicles. On the other hand, this capability may become their serious disadvantage during the landing if their spoilers or other available aerodynamic deceleration devices become inoperable in flight (cases which do not happen so often, but are definitely known in practice). Not being able to extend spoilers and dissipate the excess energy quickly enough during the final approach, a sailplane may fly over the whole available landing ground and finish up in front of the obstacles on its other end, with still too much energy to land and not enough to fly over them.

One of the known operational techniques that can be used to face this problem is the sideslipping during the final approach phase. During this intentionally uncoordinated flight, additionally generated sideforce will increase the overall drag. Principally, like with spoilers, this drag component will also dissipate additional quantity of energy and help shorten the approach distance. But this technique requires a certain amount of skill. For example, in case of a not too experienced pilot forced to land on a narrow countryside field, improper estimation of the actual flight direction while watching sideways during this maneuver, may finally place him in front of a wrong field, with no engine to help him go around and correct the error.

Besides this classical technique, in a certain number of papers the oscillating final approach patterns without sideslipping, performed in a vertical plane, have been considered as another potential option with the aim to minimize the landing distance in the case of the aerodynamic decelerating devices failure. In order to emphasize a rather high complexity level of such kind of calculations, one of them, performed for the Vuk-T sailplane [6], [7], will be presented here very briefly.

This method treated the problem of minimizing the landing approach distance as an optimal control problem, where the initial and the terminal states were based on recommendations from [2]. The lift coefficient variation was established as a variable of the control function $u(t)$ according to [3] and the maximum lift coefficient value of 1.78 for the Vuk-T was applied. Since the total time of the final approach, originally denoted as t_k, is initially unknown, calculations were done in normalized time τ, introducing another control parameter α, where $t = \alpha \cdot \tau$, $0 \le t \le t_k$, and $0 \le \tau \le 1$. Path for the minimum landing distance was obtained through an iterative calculation process, where the point was to determine such function $u(t)$ and an α that will minimize the so called performance index I, which is subjected to the dynamic, initial and terminal state constraints. Index I included the integral interior penalty functions [1] for the minimum speed and the height constraints, combined by the empirical fixed constraint factors. The problem was solved using a gradient projection algorithm [4], which incorporated conjugate directions of search for a rapid convergence of the solution. Those calculations were done in Fortran 77 in a double precision mode. Flight path obtained by these calculations is shown in Fig. 1.

Received: September 2007, Accepted: October 2007.
Correspondence to: Dr Ivan Kostić, Assistant Professor
Faculty of Mechanical Engineering,
Kraljice Marije 16, 11120 Belgrade 35, Serbia
E-mail: ikostic@mas.bg.ac.yu

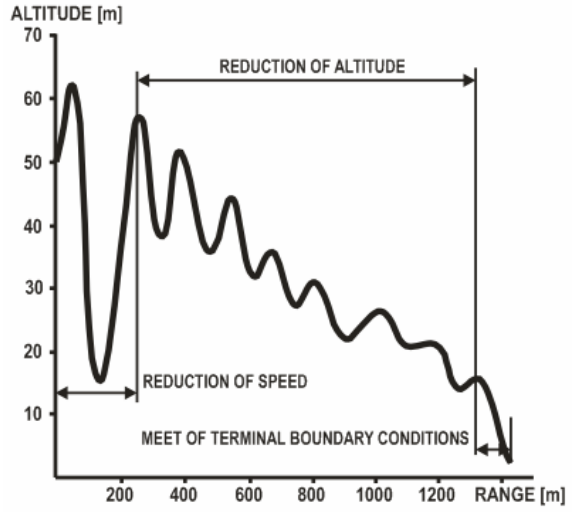

Figure 1. Minimized Vuk-T final approach path, obtained by calculations in [7]

The result of this obviously quite complex calculus is an unevenly oscillating flight path, which does give an effective reduction of the approach distance. A practical problem associated with it is that it would require exceptional piloting skills to be accurately replicated under operational conditions. If only several flying errors were accumulated, its advantages could be lost to a large extent and a pilot, attempting to land on a short terrain, could easily find himself landing at its end (and again - without an engine to help him go around and correct the error). Also, the last part of that flight path is flown oscillating at around minimum speeds at very small heights, when any sudden change of the wind speed under real life conditions may stall the sailplane and cause a disaster.

Quite opposite to the previous example, the primary aim of this paper is to investigate the possible approach distance reduction techniques (rather than focusing on the distance minimizing) through very simple speed variations with constant periods and speed amplitudes, which could be easily, safely and quite accurately performed by the pilots of average flying skills. The second aim is to perform the calculations using an algorithm that is as simple as possible, but sufficiently accurate for the required purposes. (It should be kept in mind that the primary end-users of these calculations should be the sailplane pilots, rather than highly trained engineers or programming experts.)

Suppose that a sailplane pilot, with just a general knowledge of informatics and mathematics, could be able to perform such calculations using a custom written computer program which would not require sophisticated coding skills or recompiling, for example, the spreadsheet-type program. (The use of genetic algorithms to solve this kind of problems would presently be a true challenge for engineers and mathematicians, but the idea of treating the problem in this paper is quite opposite.) In such case, a pilot would have an opportunity to experiment with the data for other sailplanes, or even do major editing, for example, assigning some different laws of speed variation or combining them for different portions of the path. This way, he could define several efficient approach paths for the sailplane he flies in advance, for the eventual case of spoilers becoming inoperable in flight. The necessary input parameters could be obtained from the sailplane manufacturers, operation manuals supplied with the sailplanes, or from other available resources, primarily the Internet.

Such an algorithm, based on a rather simple but efficient iterative approach, has been developed and presented in this paper. To stay compatible with the calculations done in [7], the Vuk-T sailplane has also been used for the analyses. Also, the initial and terminals states for the calculations are based on the same references cited for their determination in [7].

2. CALCULATION PROCEDURE

The sailplane configuration in final approach for these calculations is gear-down and spoilers-in, corresponding to the posted problem. According to the flight test measurements performed on the Vuk-T sailplane prototype at the Flight Test Center VOC-Batajnica, the polar curve for this configuration is defined by the equation:

$$C_D = 0.01756 - 0.0095 C_L + 0.021 C_L^{\,2} \ , \qquad (1)$$

where C_D and C_L are the drag and the lift coefficients, respectively. Like in [7], in this paper it will also be assigned that the nominal mass of the sailplane in flight is $m = 320\,\text{kg}$, wing area is $S = 12\,\text{m}^2$, and that the air density is $\rho = 1.225\,\text{kg/m}^3$. Using these values and (1), it can be calculated that the maximum glide ratio for this configuration is $(L/D)_{\max} = 34.59$ and the speed that corresponds to it is $V = 77.99$ km/h (for the gear-up configuration these values are different; the speed will additionally differ if some other reference mass is selected). For the default glide regime, which will be used for comparisons with approaches based on harmonic velocity variations, the rounded value of $V = 80$ km/h will be applied, for which the glide ratio is $L/D = 34.52$.

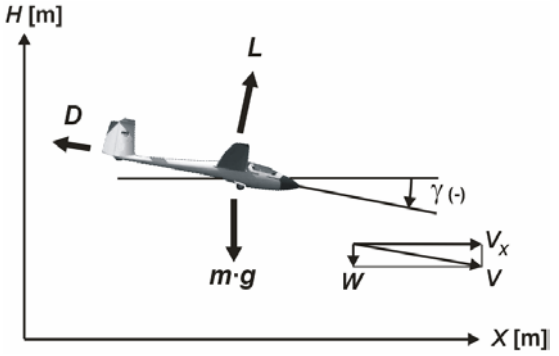

Figure 2. Notation for the forces and components of speed used in the approach path calculations

Neglecting rotation dynamics and assuming that the wind speed is equal to zero, equations of motion [5] for the purpose of these calculations (see also Fig.2. for the notation applied) can be rewritten as:

$$m\frac{\mathrm{d}V_X}{\mathrm{d}t} = -D\cos\gamma - L\sin\gamma\,, \tag{2}$$

$$m\frac{\mathrm{d}W}{\mathrm{d}t} = -mg - D\sin\gamma + L\cos\gamma\,, \tag{3}$$

$$\frac{\mathrm{d}X}{\mathrm{d}t} = V_X\,, \tag{4}$$

$$\frac{\mathrm{d}H}{\mathrm{d}t} = W\,, \tag{5}$$

$$\tan\gamma = \frac{W}{V_X}\,, \tag{6}$$

where the lift and the drag forces are:

$$L = C_L \cdot \frac{1}{2}\rho V^2 \cdot S\,, \tag{7}$$

and

$$D = C_D \cdot \frac{1}{2}\rho V^2 \cdot S\,. \tag{8}$$

In this paper the speed variations in final approach will be assigned using the following cosine law:

$$V = V_{AV} - \Delta V \cos\left(\frac{2\pi}{T}t\right) \tag{9}$$

in which V_{AV} represents the average speed, ΔV is the half-amplitude, T is the period, while time t is the independent variable.

For all presented cases, the glide path angles are smaller than ten degrees, so the small angle approximations may be applied. Thus, with the path angle γ expressed in radians, (2) and (3) can be simplified as:

$$m\frac{\mathrm{d}V_X}{\mathrm{d}t} = -D - L\cdot\gamma \tag{10}$$

and:
$$m\frac{\mathrm{d}W}{\mathrm{d}t} = -mg - D\cdot\gamma + L \tag{11}$$

It should be noted that all variables on the right hand-side of (2) and (3), or (10) and (11), with such an assigned speed variation law, are also time dependant.

First iteration step

The lift coefficient variation with time along the flight path is initially estimated from the equation:

$$C_L(t) = \frac{2\cdot m\cdot g}{\rho\cdot V(t)^2\cdot S} \tag{12}$$

using (9) to define speed changes. After that, the time dependant drag coefficient is calculated using (1). Both in this and all the following iterations, the time step of $\Delta t = 0.1$ s for numerical analyses proved to be quite satisfactory. It should be noted that the equation (12) is actually obtained from (11), omitting the product $D\cdot\gamma$ and assuming that $\mathrm{d}W/\mathrm{d}t = 0$. In usual sailplane descents, products $D\cdot\sin\gamma$ are about 1000 times smaller than $L\cdot\cos\gamma$, thus omitting $D\cdot\gamma$ does not affect the accuracy noticeably. On the other hand, for the here applied cosine speed changes, the assumption $\mathrm{d}W/\mathrm{d}t = 0$ is not true, but it has been taken as an intentional "sacrifice" in the first step of the calculations.

Lift and drag forces are then evaluated using (7) and (8). To a first approximation, it may be assumed that $\mathrm{d}V_X/\mathrm{d}t \approx \mathrm{d}V/\mathrm{d}t$. Since the variation of $V(t)$ is a known differentiable function, $\mathrm{d}V/\mathrm{d}t$ can be obtained both numerically and analytically (doing it both ways and comparing the results could be one of the verifications whether Δt is selected adequately). The initial estimate of the flight path angle γ can now be obtained directly from (10):

$$\gamma(t) = -\frac{m(\mathrm{d}V/\mathrm{d}t) + D(t)}{L(t)}\,. \tag{13}$$

The velocity components are determined as:

$$V_X(t) = V(t)\cdot\cos\gamma(t)\,, \tag{14}$$

$$W(t) = V(t)\cdot\sin\gamma(t)\,. \tag{15}$$

In the sense of numerical calculations, time derivatives at the "*i*"-th time step can be obtained as:

$$\left(\frac{\mathrm{d}V_X}{\mathrm{d}t}\right)_i = \frac{(V_i - V_{i-1}) + (V_{i+1} - V_i)}{2\cdot\Delta t}\,, \tag{16}$$

$$\left(\frac{\mathrm{d}W}{\mathrm{d}t}\right)_i = \frac{(W_i - W_{i-1}) + (W_{i+1} - W_i)}{2\cdot\Delta t} \tag{17}$$

(this approach proved to be quite satisfactory using the 0.1 second time step).

Second iteration step

Equation (12) for the lift coefficient is now upgraded, this time including values obtained from (17):

$$C_L(t) = \frac{2\cdot m\cdot(g + \mathrm{d}W/\mathrm{d}t)}{\rho\cdot V(t)^2\cdot S}\,, \tag{18}$$

while (13) is upgraded using the values obtained by (16):

$$\gamma(t) = -\frac{m(\mathrm{d}V_X/\mathrm{d}t) + D(t)}{L(t)}\,. \tag{19}$$

Lift, drag, and the velocity components with their derivatives are then recalculated applying the same algorithm as in the first iteration step, but including the refined values obtained by (18) and (19).

Third iteration and further iteration steps

The whole procedure is repeated using $\mathrm{d}V_X/\mathrm{d}t$ and $\mathrm{d}W/\mathrm{d}t$ from the previous steps, and theoretically speaking this calculation process could be repeated as many times as necessary.

After the desired level of accuracy has been achieved, the $X(t)$ and $H(t)$ coordinates, which determine the flight path profile, are calculated by numerical integration of $V_X(t)$ and $W(t)$ from the last iteration step with respect to time (coming out from (4) and (5)), using initial conditions $X(0) = 0$ m and $H(0) = 50$ m for all the cases considered in this paper. The length of the flight path $P(t)$ is obtained by numerical integration of the total velocity $V(t)$.

To quantify the obtained accuracy, results from the last iteration step of the final approach calculations were substituted in full equations (2) and (3). Differences between the left and the right-hand sides, calculated at each time step, were then compared with the calculated drag force in case of (2) and lift force in case of (3). Limit for the so defined relative errors, which could be accepted for practical considerations, was established at the order of 1% or smaller. The presented algorithm has shown very high convergence rate, since practically all analyzed cases with the cosine speed variations have fulfilled this requirement after only three iteration steps. The only exception was the one denoted as "case 3" (see next chapter, Fig.6.), where the fourth step was introduced to reduce the maximum relative error from 2.2% to 1.2% in equation (2). Since the differences between the calculated X and H values in the third and fourth step were of the order of centimeters, it has been assumed that any further accuracy improvements would be unnecessary from the practical point of view.

Terminal state is reached at the $H \approx 1$ m and $V = 72$ km/h. Thus, besides the final approach, the round-out phase and the hold-off phase also had to be calculated for the default case, and cases 1 and 4 (see next chapter), while for the other two approaches the velocity amplitudes and the corresponding periods have been selected in a way that the round-out phase is the integral part of the final approach flight segment.

The round-out phase of landing

In practical calculations it is usual to treat the round-out phase path as a circular arc, so its $R = \text{const.}$, through which the approach speed V_{AP} changes are negligible. On the other hand, changes of the load factor $n = L/(m \cdot g)$ are not. Radius of such modeled round-out phase can be determined from the equation:

$$R = \frac{{V_{AP}}^2}{g} \cdot \frac{1}{n - \cos\gamma}, \tag{20}$$

where n is the load factor at the end of this phase. For both mentioned cases, the reasonable value $n = 1.05$ has been assigned. Total variations of the height and the horizontal distance through the round-out phase are:

$$\Delta H = -R(1 - \cos\gamma), \tag{21}$$

$$\Delta X = -R\sin\gamma \tag{22}$$

(having in mind the assumed convention for the sign of the flight path angle).

The hold-off phase of landing

The hold-off phase has been modeled in the same way for all analyzed cases, through which the speed is gradually reduced to the intended touchdown value of $V_T = 72$ km/h. Although for $m = 320$ kg, the Vuk-T's stalling speed is $V_{\text{stall}} = 55.7$ km/h km/h, it should be noted that for many modern sailplanes, decelerating down to the V_{stall} would lead to the tail-first touchdowns (simulated case shown in Fig. 3), which can cause the structural damage.

Figure 3. The DG-100 sailplane tail-first touchdown at V_{stall} (flight simulation for the visual presentation of the problem performed using the MS-FS9)

Although under operational conditions there is usually a small loss of height through this phase, and strictly speaking the rate of descent is not exactly zero, the equation of level flight with center of gravity at a constant average height $H \approx 1$ m to calculate its length can be used without any penalties. Substituting $\gamma = 0^{\circ}$ in (2), it becomes:

$$m\frac{\mathrm{d}V_X}{\mathrm{d}t} = -D = m\frac{\mathrm{d}V}{\mathrm{d}t} \tag{23}$$

and thus:

$$\frac{\mathrm{d}V}{\mathrm{d}t} = -\frac{\rho \cdot V^2 \cdot C_D \cdot S}{2m}. \tag{24}$$

Initial condition is defined by V at the end of round-out phase (parameters at this point will be denoted using the asterisk symbol "(*)" in the following analyses), and for each consecutive time step speed reduction is calculated using (24), the new C_L for the reduced speed is obtained from the equation of level flight, while the corresponding C_D is calculated using (1). The iteration process is repeated until $V_T = 72$ km/h is reached. Distance X flown in this phase is obtained by the integration of speed with respect to time, and for this phase, the horizontal distance is equal to the path length.

The ground roll after touchdown is not considered in this paper, because theoretically speaking, after the same terminal state parameters have been reached, ground rolls for all analyzed cases must be exactly the same.

3. RESULTS AND DISCUSSION

For all analyzed cases, the initial (energy) state condition is defined by the height of $H = 50$ m above the terrain and the speed of $V = 80$ km/h, while the

terminal (energy) state is defined by $V = 72$ km/h and $H \approx 1$ m. Also, wind effects are not considered in this paper and the sideslip is excluded. The reference, i.e. the default linear flight path, flown at the constant speed of $V = 80$ km/h , has been selected for the comparisons with paths based on the cosine law speed variations. Because the assigned initial and terminal states must apply for the reference path as well, the 80 km/h = const case is the only one that satisfies the initial condition requirement. On the other hand, this is practically the best glide ratio speed for the analyzed sailplane configuration, and it is known that any other constant approach speed selected would give a shorter approach distance. But then, to preserve the consistency of the analyses, all cosine approaches analyzed in this paper would also have to commence at the initial state which is defined by this different speed (instantaneous velocity changes are not possible), and results obtained for such paths would be different as well. Before commencing a final approach, the most common practice is to fly a sailplane at the best glide ratio – so the here applied selections of the initial state and reference path speed are closest to the real life situations.

The four typical cases, selected for presentation in this paper, are shown in Fig.s 4 ÷ 7. In all cases the speed initially increases from 80 km/h.

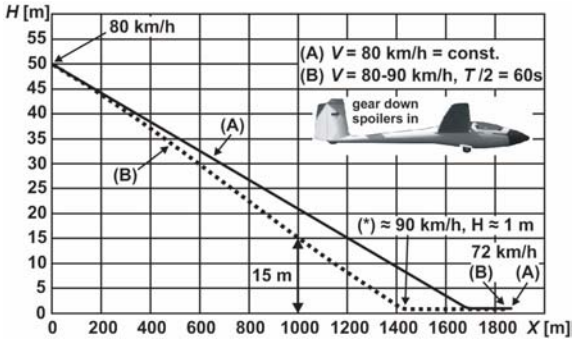

Figure 4. Case 1: distance reduction X_A - X_B = 33.1 m

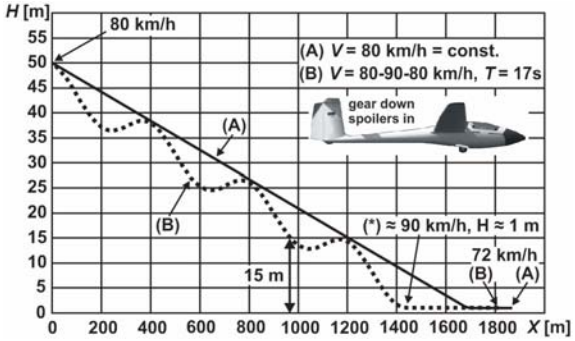

Figure 5. Case 2: distance reduction X_A - X_B = 56.7 m

Table 1. *L/D* ratios for some characteristic speeds

Configuration: gear down, spoilers in, m = 320 kg			
V [km/h]	80	90	110
L/D	34.5	32.7	26.0

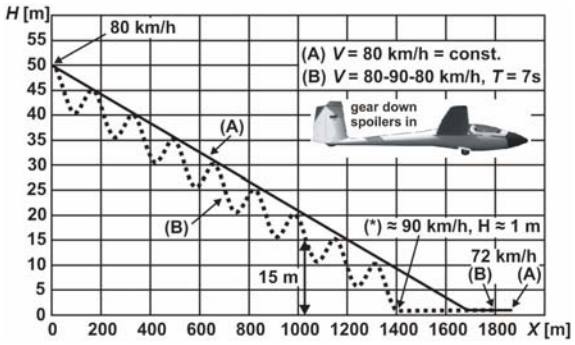

Figure 6. Case 3: distance reduction X_A - X_B = 78.9 m

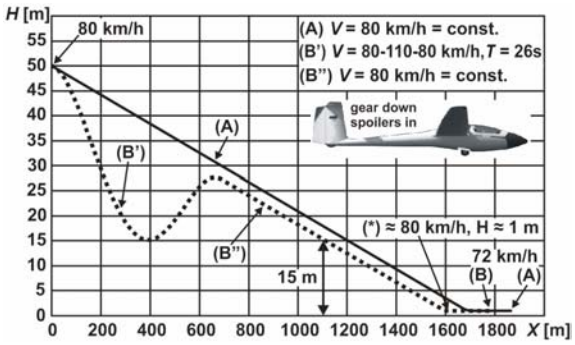

Figure 7. Case 4: distance reduction X_A - X_B =101.8 m

Table 2. The most relevant flight path parameters

Para-meter	Default case	Case 1	Case 2	Case 3	Case 4
ΔX [m]	/	33.1	56.7	78.9	101.8
D^*_{AV} [N]	90.9	92.1	93.1	94.1	103.9' 96.6$_{all}$
T [s]	/	120	17	7	26
ΔV [km/h]	0	10	10	10	30
$\Delta\, L/D$	0	-5.2%	-5.2%	-5.2%	-24.6%
γ [°] change	none	-2.12 -1.54	-4.69 +1.31	-9.02 +5.62	-7.76 +4.07
n change	none	0.999 1.001	0.956 1.049	0.743 1.298	0.943 1.078

** - distance averaged drag force D_{AV} shown in this table does not include the hold-off phase*

For the clarity of presentation, the applied scales for height H and horizontal distance flown X in Fig.s 4 ÷ 7 had to be substantially different. Due to that, the graphical appearances of the paths are largely distorted with respect to their true forms. For example, the calculated horizontal distance of the path up to the end of the round out phase (parameters denoted by the (*) symbol) for the *default case* (denoted as "(A)" in all graphs) is $X(*) = 1706.0$ m, while the path length obtained through numerical calculations is $P(*) = 1706.7$ m. Thus the difference between them is

only 70 cm, while the path appearance in the diagrams suggests that it should be much larger. A simple approximate verification could be done by neglecting the path curvature of the round-out phase and knowing that $\Delta H = 49$ m: $\sqrt{1706^2 + 49^2} = 1706.7$ m.

The same applies for the oscillating paths. For example, for the case 4, the calculated difference between $P(*)$ and $X(*)$ is only about 2.5 m, while the appearance of diagram also suggests much larger value. For the verification, let us just approximate the path of the first half of the period T with a straight line - it will be only some 1.6 m longer than the horizontal distance X (see Fig.s 7 and 8): $\sqrt{390^2 + 35^2} = 391.57$ m.

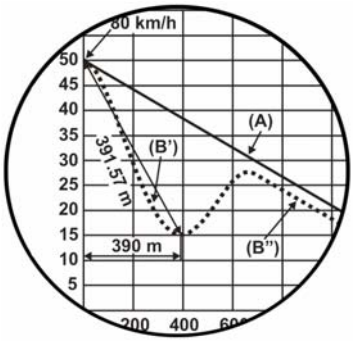

Figure 8. Even a simplified calculation of the path length leads to a conclusion that the flight path curvatures are actually very small

Proceeding with such simple analyses would finally lead to a very important general conclusion that the cosine path curvatures are actually very small. Thus, the fact alone that instead of linear, the curved oscillating paths are flown, does not contribute significantly to the overall X distance reduction.

For all presented cases the distance averaged drag forces D_{AV} were calculated, first by obtaining the sums of products of the drag forces and the path lengths for each time segment, and then dividing them with the total path lengths (the hold-off phase was not included in these calculations). As can be seen from Table 2, progressive increase of those values is proportional to the larger X distance reductions. This is quite logical, knowing that the dissipation of energy between the initial and the terminal energy states (same for all cases) is obtained through the work done by the drag force along the flight path. Thus increasing the drag (rather than curving the path in the vertical plane) is the primary aim in attempts to shorten the landing approach distance from $H = 50$ m (making full turns to reduce altitude from such a small height is strictly forbidden).

According to Fig.s 4 ÷ 7 and Table 2, there are obviously two ways to increase the drag. The first one is to alter the speed as much as possible from the best glide ratio speed (but to a reasonable extent and through a safe maneuver, because the most important pilot's aim is to stay alive). By increasing the speed from 80 km/h to 110 km/h, the glide ratio drops from 34.5 to 26.0 (see Table 1.), so for the same amount of the generated lift, the more drag is produced. Applied only in a single oscillation with quite large period of $T = 26$ s, in case 4, such maneuver has generated the X distance reduction of more than a hundred meters, which is the largest value of all presented cases. (This particular case could be further developed to give even higher reductions.)

To define the second influential factor on the drag increase, we will focus on cases 1, 2 and 3. In all of them, the speed variations are the same, between 80 and 90 km/h, which causes rather small changes in L/D ratio between 34.5 and 32.7, as shown in Table 1. On the other hand, their periods are substantially different. In case 1, an extremely large period of 120 seconds has been applied in only a half period oscillation, practically simulating an almost uniform speed increase and gave rather small $\Delta X = 33.1$ m. (With certain alternations in general case assignments, it could give even higher distance reductions, practically as in case 2., but such analyses presently exceed the scope of this paper.) The second case has much shorter period of $T = 17$ s, and gives higher value of $\Delta X = 56.7$ m. Following this trend, the case 3 with very short period of $T = 7$ s gives even larger $\Delta X = 78.9$ m. A conclusion is that the shorter periods of oscillations, as a second influential factor, lead to the additional increase of the average drag force.

As seen in Table 2, the shortening of the period consequently induces larger variations of the load factor. Also, those variations are not symmetrical, i.e. the increase of n at the local path minimums is larger than its decrease at the local maximums (this can clearly be seen for the cases 2, 3 and 4, while for the case 1 variations are too small to be shown within the significant number of digits). Increased n is the consequence of increased lift force and consequently increased drag as well, and vice versa. More cycles of such asymmetrical load factor variations during the final approach would generate an overall drag increase as a final consequence.

Combining these two influential factors should be done carefully for operational applications. For example, large speed amplitudes with very short periods can quickly become very unpleasant for the pilot and disable him to perform the assigned approach properly. Also, one of the shortcomings of here presented cosine approach examples is that the standard 15 m obstacle overshooting distances are moved some 200 meters towards the starting point, compared with the default path. It should be emphasized that the given examples have been selected primarily to clearly impose the most important issues of the analyzed physical problem, and not to determine an optimum solution or the largest possible approach distance reduction for a given sailplane. As already mentioned, applying these techniques, even larger ΔX values can certainly be achieved; also, using the cosine laws for speed variations with speed initially decreasing, the obstacle overshooting distance could be enlarged, etc. Another goal that has been set is that performing such paths must be simple and safe. In that sense, the approach distance reductions of the order of a football field length or higher are definitely not negligible for a sailplane pilot,

who is not able to use spoilers in final approach and is forced to land on a short countryside field, where practically every meter of the shortened flight can make a crucial difference between the successful landing and a disaster.

4. CONCLUSION

Algorithm developed for the calculation of the landing approach flight paths has shown high stability and convergence rate, and has enabled very efficient determination of many possible solutions for the posted category of problems. The four typical solutions have been selected for the presentation in this paper, with an aim to emphasize the influence of certain factors on the possibility of the approach distance reduction in cases when spoilers become inoperable.

It has been shown that conversion from linear to curved oscillating paths, by itself, does not contribute to any significant reduction of the horizontal distance flown, because the effective curvatures of the paths are small. On the other hand, the consequence of flying along such paths is the drag increase, generated by two sources. The first is departing from the optimum glide ratio speed to a reasonable extent, when the glide ratio decreases, and more drag is generated for the given amount of lift. The second is decreasing the period of oscillations and thus increasing the total number of oscillations during the final approach. The asymmetric change of the load factor at local path minimums and maximums is generated and additional drag is gathered.

Safety and simplicity are very important requirements in performing the paths based on the here presented principles. Possible approach distance reductions that can be achieved through them, although generally smaller than by the sideslipping or distance minimizing techniques, can be extremely useful under operational conditions, when spoilers or other aerodynamic decelerating devices are not available because of some technical problem.

REFERENCES

[1] Ladson, L.S., Waren, A. D., Rice, R. K.: An Interior Penalty Method for Inequality Constrained Optimal Control Problems, IEEE Transactions on Automatic Control, Vol.12, IV, pp. 388-395, 1967.

[2] Metzger, D.E., Hedrik, J.K.: Optimal Flight Paths for Soaring Flight, Journal of Aircraft, Vol. 12, No 11, pp. 867-871, 1975.

[3] Pierson, B. L.: Maximum Altitude Sailplane Winch-Launch Trajectories, Aeronautical Quarterly, Vol. 28, pp. 75-84, 1977.

[4] Pierson, B. L.: Panel Flutter Optimization by Gradient Projection, International Journal for Numerical Methods in Engineering, Vol. 9, pp. 271-296, 1975.

[5] Roskam, J., Chuen-Tau, E. L.: *Airplane Aerodynamics and Performance*, DARcorporation, Kansas, 1997.

[6] Stefanović, Z, Cvetković, D.: Minimizing Landing-Approach Distance for a VUK-T Sailplane, FME Transactions, Vol. XXV, issue 1, pp. 39-41, 1996.

[7] Stefanović, Z, Cvetković, D.: Minimum Landing-Approach Distance for a VUK-T Sailplane, 20th International Council of Aeronautical Sciences (ICAS) Congress, proc. pp. 1061-1064, Sorrento, Italy, 1996.

УТИЦАЈ ПРОСТИХ ХАРМОНИЈСКИХ ПРОМЕНА БРЗИНЕ НА ОБЛИК И ДУЖИНУ ПРИЛАЗНЕ ПУТАЊЕ ЈЕДРИЛИЦЕ ВУК-Т

Зоран Стефановић, Иван Костић

Уколико из било ког техничког разлога ваздушне кочнице престану да функционишу током лета, најкритичнија фаза у процедури слетања једрилице је финални прилаз. Поред лета са бочним клизањем, када се дисипација енергије врши кроз повећање бочне силе отпора, друго могуће решење овог проблема је понуђено у литератури, где је показано да се дужина прилаза може минимизирати применом сложених осцилаторних путања лета. Међутим, лет по таквим путањама захтева изузетно летачко умеће. Насупрот томе, у овом раду извршена је анализа једноставнијих прилазних путања, базираних на хармонијским променама брзине, које је много лакше оперативно репродуковати у лету. У раду је приказан прорачунски алгоритам који омогућава брзу конвергенцију решења и анализирана су нумеричка решења за неколико типичних случајева. Као пример коришћени су подаци за једрилицу Вук-Т. Добијени резултати показују нешто мања скраћења путања, али једноставност примене у пракси и већа безбедност предложених техника летења чини их корисним решењима у случају поменутих проблема.